Proceedings of the 11th World Congress on Electrical Engineering and Computer Systems and Sciences (EECSS'25)
Paris, France - August, 2025
Paper No. ICBES 200
DOI: 10.11159/icbes25.200

Brain Response to Different Pulse Width Based on Action Potential and the Effect of Sodium and Potassium Conductance on Neuron

Saeed Charbenny[1], Zhihong Huang[1]
[1]University of York
Heslington, York, United Kingdom
swd525@york.ac.uk; zhihong.huang.york.ac.uk

Abstract - Neuron action potentials (APs) represent the transition of neurons from a resting to an active state. While activation via energy deposition and mechanical waves is recognized, the underlying mechanisms remain unclear. Low-Intensity Focused Ultrasound (LIFU) enables non-invasive neuromodulation, yet its interaction with neuronal excitability and AP initiation is not fully understood. This study presents a simulation framework to investigate brain thermal responses at the AP intensity threshold across varying pulse widths (PWs), leveraging thermal modeling's higher detection sensitivity compared to experimental methods. This work investigates thermal effects at the neuronal AP threshold under LIFU stimulation. A single-cell neuron model was used to define activation thresholds, and thermal responses were simulated across three pulse widths (1, 5, and 9 ms), each applied with a 10% duty cycle (DC) and 100 Hz pulse repetition frequency (PRF). An in-lab transducer was experimentally characterized and replicated in simulation to validate acoustic and thermal behavior. The study offers a novel framework linking neuronal excitability with thermal simulation for physiologically grounded LIFU dosimetry. Temperature elevations of approximately 0.010704 °C were observed across all PW inputs when maintaining a 10% DC. For simulations with a PRF of 100 Hz, the temperature increases were 0.010704 °C, 0.010708 °C, and 0.010712 °C for 1 ms, 5 ms, and 9 ms PWs, respectively. These minimal variations suggest that under constant DC, PW duration has negligible influence on thermal elevation. In contrast, PRF had a more noticeable impact on thermal buildup. Additionally, differences in sodium and potassium conduction were observed, indicating the distinct roles of ion channel dynamics in neuronal activation. Collectively, these findings enhance our understanding of LIFU-induced neuromodulation by clarifying the relationship between thermal responses and temporal input parameters.

***Keywords*:** FUS, ultrasound, thermal, neuromodulation, action potential

1. Introduction

Low-Intensity Focused Ultrasound (LIFU) is a non-invasive neuromodulation technique that has demonstrated the capability to reversibly modulate region-specific brain activity. The term "low intensity" refers to ultrasound intensity levels that are comparable to or lower than those used in diagnostic ultrasound imaging. Numerous *in vivo* studies have shown LIFU's potential to either enhance or suppress neuronal activity without causing structural brain damage [1-7]. Compared to conventional neuromodulation techniques—such as deep brain stimulation (DBS), transcranial current stimulation (tCS), and transcranial magnetic stimulation (TMS)—LIFU offers several significant advantages. For instance, DBS requires invasive surgical procedures, introducing risks such as infection and immune response [8]. Meanwhile, both tCS and TMS are limited by their lack of spatial specificity and reduced ability to penetrate and effectively target deep brain regions [1].

LIFU stimulation is thought to activate neurons through two primary mechanisms: mechanical and thermal interactions. The first mechanism involves mechanical effects, such as the activation of mechanosensitive ion channels. These channels convert mechanical forces into electrical signals and are embedded within the cell membrane. Among them, transient receptor potential (TRP) channels are particularly notable, as they respond to membrane stretching and serve as key mediators of mechanotransduction [9]. The second mechanism involves thermal effects. In one study, a temperature increase of up to 2 °C was induced, and suppression of somatosensory evoked potentials was observed to correlate closely with the thermal time course, suggesting a thermally mediated neuromodulatory effect [10].

Simulation is a powerful tool for detecting subtle changes in brain regions that are sensitive, complex, and located deep within neural tissue. Neurons are the primary targets of LIFU exposure. Although LIFU has been shown to successfully induce neuromodulation, the underlying neurophysiological mechanisms of focused ultrasound (FUS)-induced neuronal activation remain unclear. Current thermal imaging techniques lack the sensitivity required to detect the minimal temperature

changes associated with low-intensity ultrasound exposure. In contrast, simulation provides a valuable alternative by enabling the precise quantification of subtle thermal effects under various stimulation parameters.

This study presents a novel computational framework that integrates single-neuron modelling using MetaNeuron [11] with high-resolution acoustic and thermal simulations conducted in Sim4Life [12]. By combining electrophysiological models with ultrasound simulation, this approach bridges the gap between neuronal activity and acoustic energy delivery, offering a more comprehensive understanding of the biophysical interactions underlying LIFU-induced neuromodulation.

2. Methods

2.1 Action potential

Simulation provides a valuable opportunity to visualize neuronal behavior both at rest and under various forms of stimulation. It enables researchers to determine when a neuron is likely to become excited or inhibited based on specific stimulus parameters. In this study, MetaNeruon [11] was used as the simulation tool to model neuronal responses under different stimulation conditions. MetaNeuron is based on the foundational model developed by Hodgkin, Huxley, and Katz [13], which describes the ionic mechanisms underlying the initiation and propagation of action potentials. Under typical conditions of neuronal activation, a threshold phase precedes depolarization. This threshold represents the minimum membrane voltage required to trigger an action potential. Neuronal excitation depends on several factors, including stimulus amplitude, stimulus duration, and the conductance of various ion channels. In the initial simulation settings, the stimulus was configured with a width of 0.1 ms and an amplitude of 65 μA. Figure 1 illustrates the resulting action potential generated under these baseline conditions.

2.2 Lab transducer recordings

Simulation of the transducer was based on an experimental in-lab setup designed to replicate real-world acoustic conditions. The experimental configuration included a focused ultrasound (FUS) transducer, a 0.2 mm needle hydrophone, and an amplifier (Precision Acoustics Ltd., Dorchester, Dorset, UK). The transducer operated at a center frequency of 0.667 MHz, with a focal length of 75 mm and an active aperture diameter of 60 mm [14]. To measure the acoustic pressure, the transducer was submerged in a water tank, and a needle hydrophone was positioned at the focal point. The transducer was driven by a function generator (KEYSIGHT 33220A), which produced an input voltage of 70 mV at 0.667 MHz. This signal was subsequently amplified using a radio frequency (RF) amplifier, delivering an output of 1 W to drive the transducer. The hydrophone was mounted on a three-axis positioning system and placed precisely 75 mm from the transducer to align with the focal zone. It was connected to a DC coupler (DCPS160), which interfaced with a PicoScope for data acquisition. Recorded signals were visualized and analyzed on a connected computer, enabling accurate characterization of the pressure field generated by the transducer.

The conversion from voltage to pressure are achieved by the following equation:

$$Pr = \frac{V}{S} \tag{1}$$

Where:
Pr: Acoustic pressure (Pascal)
V: Hydrophone voltage output (Volt)
S:Hydrophone sensitivity (V/Pa)

2.3 Simulation of transducer

The simulated transducer was modeled to replicate the characteristics of the experimental transducer. Similar to the laboratory setup, the simulation featured a single-element focused ultrasound (FUS) transducer and was conducted using the Sim4Life software platform (Sim4Life, Zurich, Switzerland) [12]. The simulated transducer had a curvature radius of 60 mm, an operating frequency of 0.667 MHz, and an aperture width of 70 mm, closely matching the physical parameters of the experimental device to ensure consistency in acoustic behavior.

2.4 Simulation material settings

Sim4Life provides detailed anatomical models for simulation, and the model used in this study was imported into the Sim4Life environment. The anatomical model represents a 34-year-old male, with a height of 1.77 m and a weight of 70.2 kg. The head voxel resolution consisted of 0.5 mm × 0.5 mm pixel spacing and a slice thickness of 0.5 mm. The simulated transducer was positioned on the front-right side of the head model to replicate the experimental setup. Table 1 summarizes the material properties assigned to the various tissues used in the simulation.

Table 1: Simulation material properties for acoustic and thermal

Materials	Speed of sound m/s	Mass Density kg/m^3	Specific Heat Capacity J/kg/K	Thermal Conductivity W/m/K	Heat Generation Rate W/kg
Compact Skull	2813.69	1908	1312.83	0.32	0.154869
Cancellous skull	2117.53	1178.83	2274	0.3125	0.464607
Cerebrospinal fluid	1504.5	1007	4095.5	0.573333	0
Dura Matter	1500	1174	3364	0.44	5.88502
Brain (Grey matter)	1500	1044.5	3695.8	0.547	15.5391
Brain (White matter)	1552.5	1041	3582.8	0.481	4.32057
Commissura Anterior	1552.5	1041	3582.8	0.481	4.32057
Midbrain	1546.32	1045.5	3630	0.51325	11.3666
Thalamus	1500	1044.5	3695.8	0.547	13.9282
Pons	1546.32	1045.5	3630	0.51325	11.3666
Hypophysis	1500	1053	3687	0.514	13.7059
Hypothalamus	1500	1044.5	3695.8	0.547	15.5391
Hippocampus	1500	1044.5	3695.8	0.547	15.5391
Spinal Cord	1542	1075	3630	0.51325	2.48307
Cerebellum	1537	1045	3653	0.506	15.668
Medulla Oblongata	1546.32	1045.5	3630	0.51325	11.3666
Commissura Posterior	1552.5	1041	3582.8	0.481	4.32057
Pinal Body	1500	1053	3687	0.514	13.7059

2.5 Thermal monitoring

The simulation setup was first validated by comparing it against an established therapeutic protocol before proceeding with subsequent research simulations. Specifically, the reference treatment utilized High-Intensity Focused Ultrasound (HIFU) to deliver energy. In this treatment, the FUS system delivered a power of 648 Watts and a total energy of 8,424 Joules [15].

After the confirmation of power and energy of the treatment procedure, intensity was needed for simulation replication of treatment. Intensity can be determined with the equation that relates power to the spatial distribution of energy:

$$I = \frac{(P)}{(A)} \tag{2}$$

Where:

I: Intensity in Watt/cm^2 or Watt/m^2

P: Power in Watt
A: Focused ultrasound area in cm^2 or m^2

Equation 2 calculates the intensity at the focal area and requires the focal zone's cross-sectional area as an input. Since the treatment procedure did not specify the focal area, we approximated it based on the focal dimensions of the experimental simulation transducer. By calculating the treatment intensity and ensuring it matched that of the simulation, the simulation parameters were validated and could be confidently applied to subsequent experimental conditions. It is important to note that the HIFU treatment parameters were used solely for validation purposes before conducting the various LIFU simulation scenarios.

Calculating the intensity or pressure at which the neuronal activation threshold occurs was essential for assessing the effects of our experimental simulation. The threshold voltage required to trigger an action potential was extracted using MetaNeuron, which allowed visualization and precise detection of this critical voltage. To relate this voltage to the ultrasound pressure, a conversion was performed using an established equation. The sensitivity of the hydrophone was determined based on the characteristics of the experimental transducer. Once the hydrophone sensitivity was identified, we were able to accurately calculate the pressure corresponding to the neuronal action potential threshold voltage.

The required pressure and intensity levels, determined based on the neuronal action potential threshold, were successfully achieved in the simulation. With this calibration, we proceeded to simulate the specified input parameters. The simulations investigated pulse widths of 1, 5, and 9 ms, each applied with a 10% duty cycle (DC) and a pulse repetition frequency (PRF) of 100 Hz for 10 seconds.

3. Results

3.1 Neuron conductance

At rest, the neuron's membrane potential was measured at –65 mV. Upon exposure to a stimulus, the neuron exhibited a pre-depolarization phase, known as the threshold phase, which precedes full depolarization. This shift in membrane potential ultimately drives the neuron to fire an action potential. Specifically, stimulation caused the membrane potential to rise from –65 mV to –58 mV, representing a 7 mV change, the voltage increase required to reach the activation threshold, as illustrated in Figure 1. All subsequent simulations were conducted using this 7 mV threshold as the baseline for neuronal activation.

Simulation allows us to evaluate how variations in ion conductance affect neuronal stimulation. In this study, the conductance's of sodium (Na^+) and potassium (K^+) ions were varied while keeping the stimulation parameters constant, with an amplitude of 65 μA and a stimulus width of 0.1 ms. As shown in Figure 1, changes in ion conductance significantly influenced the neuron's action potential dynamics. At a sodium conductance (g_Na max) of 260 mS/cm², the neuron exhibited normal action potential activation. Increasing g_Na from 260 to 930 mS/cm² caused the action potential threshold to be nearly bypassed, shortening the time between threshold and depolarization. However, further increases beyond 980 mS/cm² disrupted the balance of the depolarization phase, resulting in an unstable polarization process, as seen in Figure 1. Conversely, reducing sodium conductance below 260 mS/cm² increased the delay between threshold and depolarization, eventually preventing the neuron from firing. Under normal stimulation, the time from threshold to depolarization ranges from 0.61 ms to 1.50 ms, a difference of 0.89 ms. When g_Na was decreased to 244 mS/cm², the neuron failed to reach depolarization, but at 245 mS/cm², an action potential was successfully generated, albeit with a prolonged time from threshold to depolarization of 2.25 ms, an increase of 1.64 ms compared to the normal range.

Simulations of potassium (K^+) conductance were conducted while maintaining sodium conductance at its normal value of 260 mS/cm². Under normal conditions, potassium conductance (g_K) was set at 70 mS/cm², supporting typical action potential generation. Reducing g_K to 6 mS/cm² caused the neuron to fail to reach the depolarization stage. Although the time from threshold to depolarization decreased significantly, the neuron did not fully depolarize. Interestingly, at 7 mS/cm², rather than failing, the neuron exhibited an extended polarization period and generated a second action potential. Conversely, increasing g_K to 75 mS/cm² prevented the neuron from depolarizing, while at 74 mS/cm², an action potential was

successfully produced, but with a prolonged duration between threshold and depolarization. Specifically, the time from threshold (0.61 ms) to depolarization increased to 1.82 ms at 74 mS/cm², resulting in a 1.21 ms delay compared to normal conditions.

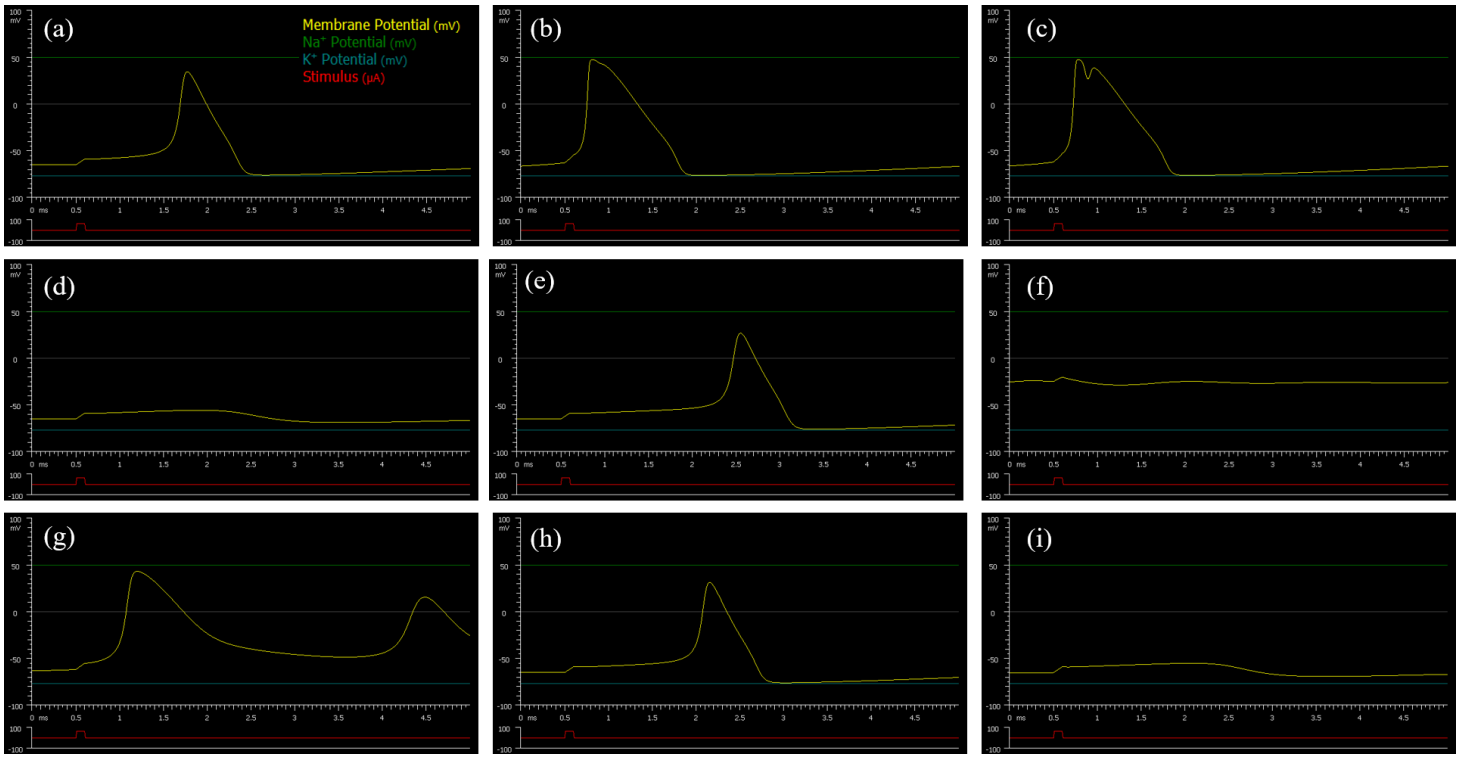

Fig. 1: (a) Action potential under normal stimulation. (b) Na^+ conductance at 930 mS/cm^2. (c) Na^+ conductance at 980 mS/cm^2. (d) Na^+ conductance at 244 mS/cm^2. (e) Na^+ conductance at 245 mS/cm^2. (f) K^+ conductance at 6 mS/cm^2. (g) K^+ conductance at 7 mS/cm^2. (h) K^+ conductance at 74 mS/cm^2. (i) K^+ conductance at 75 mS/cm^2.

3.2 Simulation of transducer and Sensitivity

Simulating neuron activation based on the action potential threshold voltage required converting voltage to pressure. This conversion was performed using Equation 1, which calculates hydrophone sensitivity and, subsequently, the pressure corresponding to the neuronal threshold voltage. Based on experimental measurements, the recorded pressure and voltage were 860 kPa and 0.8 V, respectively. Applying Equation 1 yields a sensitivity value of:
S=0.8V/860K=0.00000093 V/Pa.

3.3 Thermal simulation procedure

The validity of the simulation framework was established by aligning it with a real-life treatment procedure before conducting our experimental simulations. This validation step ensured that the outcomes of our simulations could reliably reflect actual physiological conditions. The reference treatment procedure utilized High-Intensity Focused Ultrasound (HIFU), delivering 648 W of power and 8,424 J of energy. To replicate this treatment in simulation, it was necessary to match the intensity. Equation 2 was used to calculate acoustic intensity. However, because the original treatment did not provide the focal beam area, we approximated it using the focus area dimensions from our simulation model. The intensity was then calculated as follows:

$$648 = (I)(0.1457) \Rightarrow I = \frac{648}{0.1457} = 4447.5\frac{W}{cm^2}$$

Which can express as: $44{,}475{,}000\ \frac{\mathrm{W}}{\mathrm{m}^2}$

Based on the calculated intensity, pressure was 12.030942 MPa. Validating the treatment, enabled us to simulate based on our researched parameters. From the neuron simulation, we extracted the voltage needed to cause threshold to be 7 mV. The resulted pressure was 7526 Pa, which has an intensity of 17.6 W/m^2 (0.00176 W/cm^2). The calculated pressure was:

$$V = (Pr)(S) => Pr = \frac{V}{S} = \frac{0.007}{0.00000093} = 7526\ Pa$$

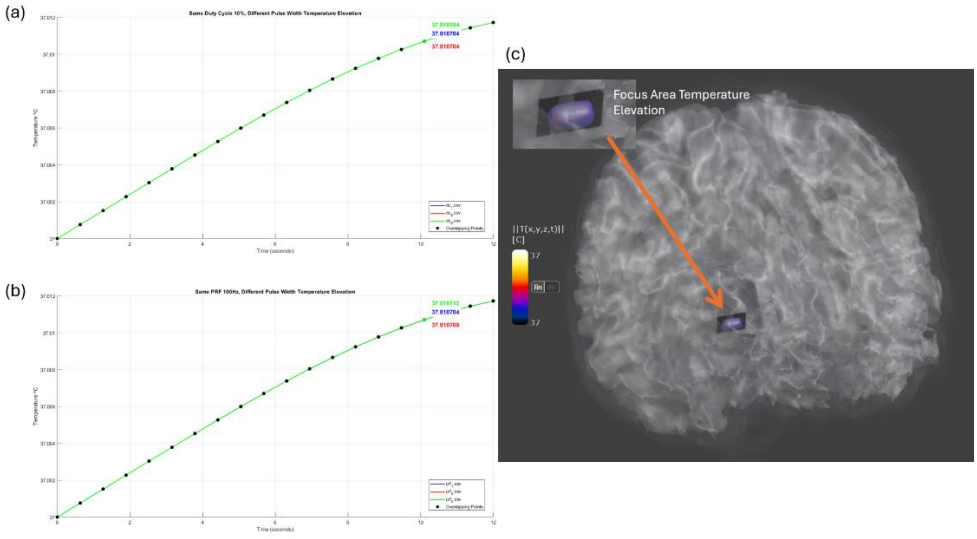

Fig. 2: (a) Temperature elevation under 10% DC for 10 seconds. (b) Temperature elevation under 100 PRF for 10 seconds. (c) Temperature elevation caused by the focused ultrasound beam.

Table 2. Temperature elevation for 1, 5, 9 ms under 10%DC and 100 PRF

Pulse Width ms	Temperature °C, 10% DC	Temperature °C, 100 PRF
1	37.010704	37.010704
5	37.010704	37.010708
9	37.010704	37.010712

Table 2 presents the thermal simulation results for pulse widths (PWs) of 1 ms, 5 ms, and 9 ms, each applied with a duty cycle (DC) of 10% and a pulse repetition frequency (PRF) of 100 Hz. Under the constant duty cycle condition, all three pulse widths produced nearly identical temperature elevations, with a peak temperature of approximately 37.010704 °C. However, when isolating the influence of pulse width under fixed PRF conditions, subtle differences in thermal response were observed. Specifically, the temperatures recorded were 37.010704 °C, 37.010708 °C, and 37.010712 °C for 1 ms, 5 ms, and 9 ms pulse widths, respectively, as illustrated in Figure 2. These results suggest that while the duty cycle is the dominant factor in thermal accumulation, increasing pulse width under fixed PRF slightly raises tissue temperature.

4.Discussion

Simulation results demonstrated that the resting membrane potential of the neuron was −65 mV. Upon stimulation with an additional 7 mV, the membrane potential shifted to −58 mV, reaching the threshold necessary to trigger an action potential. This threshold phase marks the critical transition from a resting to an active neuronal state under normal stimulation conditions. The findings indicate that a voltage change of just 7 mV is sufficient to elicit a proper neuronal response, emphasizing the high sensitivity of neuronal excitability to minimal electrical perturbations.

Simulation results highlighted the influence of sodium (Na^+) and potassium (K^+) conductance on the progression of neuronal action potentials. While stimulation parameters were held constant (65 μA amplitude, 0.1 ms pulse width, Na^+ conductance at 260 mS/cm², and K^+ conductance at 70 mS/cm²), variations in Na^+ conductance produced notable effects. Increasing Na^+ conductance to 930 mS/cm² led to a much faster depolarization, with the threshold phase nearly bypassed due to the enhanced influx of sodium ions. However, this rapid depolarization disrupted the peak potential and impaired repolarization, which may affect the fidelity of signal transmission to adjacent neurons, as illustrated in Figure 1.
Conversely, reducing Na^+ conductance progressively delayed depolarization, and at 244 mS/cm², the neuron failed to reach the depolarization threshold entirely. A minimal conductance of 245 mS/cm² still enabled successful action potential generation, though the time from threshold to depolarization increased from 0.89 ms (under normal conditions) to 1.64 ms. These results demonstrate that decreased Na^+ conductance prolongs the time required for depolarization, highlighting its critical role in maintaining both the speed and reliability of neuronal activation.

In addition to the influence of sodium conductance, potassium (K^+) conductance also significantly affects neuronal action potential dynamics. Under normal conditions, Na^+ and K^+ conductance values are set at 260 mS/cm² and 70 mS/cm², respectively. Reducing K^+ conductance below the baseline led to notable changes in neuronal response. At 6 mS/cm², the neuron failed to depolarize, whereas at 7 mS/cm², although depolarization was achieved, the repolarization phase was prolonged, resulting in the generation of a secondary action potential. Conversely, increasing K^+ conductance above the normal value impaired depolarization. At 75 mS/cm², the neuron failed to generate an action potential. However, at 74 mS/cm², successful depolarization was observed, albeit with delayed activation. The time from threshold to depolarization increased from 0.61 ms (under normal conditions) to 1.21 ms. These findings suggest that deviations from optimal K^+ conductance—whether increases or decreases—can disrupt the timing and reliability of neuronal firing, further emphasizing the delicate balance of ion channel dynamics in neuronal excitability.

The simulation demonstrated that a neuron requires only a 7 mV depolarization to initiate an action potential, which corresponds to an acoustic pressure of approximately 7526 Pa. This pressure value was used as the input for the simulated transducer to match the neuron activation threshold. Thermal simulations based on this pressure input were conducted for three pulse widths—1 ms, 5 ms, and 9 ms—each applied with a 10% duty cycle (DC). The resulting temperature elevation was consistent across all pulse widths, reaching 37.010704 °C, indicating that pulse width alone, when DC is held constant, has minimal influence on thermal accumulation. However, when the same pulse widths were simulated under a pulse repetition frequency (PRF) of 100 Hz, slight but measurable temperature variations were observed: 37.010704 °C, 37.010708 °C, and 37.010712 °C for 1 ms, 5 ms, and 9 ms respectively. These results highlight the more pronounced role of PRF in influencing thermal effects during LIFU exposure, suggesting that PRF modulation may be a more effective parameter for thermal dosing than pulse width under a fixed duty cycle.

5.Conclusion

This study presents an integrative simulation framework that combines biophysical neuron modelling with focused ultrasound (FUS) acoustic and thermal simulations. Using MetaNeuron, we identified the threshold voltage required to elicit an action potential, which was subsequently converted into an equivalent acoustic pressure to inform the ultrasound simulation parameters. To our knowledge, this represents the first in silico framework to physiologically link neuronal excitation thresholds with acoustic energy delivery in a unified and biologically informed manner. While this approach demonstrates significant potential, it also has notable limitations. MetaNeuron does not account for mechanical or biomechanical responses of neurons to ultrasound exposure, which may play a role in neuromodulation mechanisms. Additionally, although the voltage-to-pressure conversion method is a novel approach, the framework would benefit from experimental validation to ensure the accuracy of its predictions and real-world applicability.

Acknowledgements

The author would like to thank University of Dundee and York for the facilitating in achieving the research. The author would like to thank Sim4Life for the simulation software that enabled us to achieve the investigation.

References

[1] H. Baek, K. J. Pahk, and H. Kim, “A review of low-intensity focused ultrasound for neuromodulation,” *Biomedical Engineering Letters*, vol. 7, no. 2, pp. 135–142, Jan. 2017, doi: https://doi.org/10.1007/s13534-016-0007-y.

[2] F. J. Fry, H. W. Ades, and W. J. Fry, “Production of Reversible Changes in the Central Nervous System by Ultrasound,” *Science*, vol. 127, no. 3289, pp. 83–84, Jan. 1958, doi: https://doi.org/10.1126/science.127.3289.83.

[3] H. T. Ballantine Jr., E. Bell, and J. Manlapaz, "Progress and problems in the neurological applications of focused ultrasound," *J. Neurosurg.*, vol. 17, no. 5, pp. 858–876, Sep. 1960. doi: 10.3171/jns.1960.17.5.0858.

[4] H. Kim, A. Chiu, S. Park, and S.-S. Yoo, “Image-guided navigation of single-element focused ultrasound transducer,” *International Journal of Imaging Systems and Technology*, vol. 22, no. 3, pp. 177–184, Aug. 2012, doi: https://doi.org/10.1002/ima.22020.

[5] W. Lee, H. Kim, Y. Jung, I.-U. Song, Y. A. Chung, and S.-S. Yoo, “Image-Guided Transcranial Focused Ultrasound Stimulates Human Primary Somatosensory Cortex,” *Scientific Reports*, vol. 5, no. 1, p. 8743, Mar. 2015, doi: https://doi.org/10.1038/srep08743.

[6] A. Bystritsky, A. S. Korb, P. K. Douglas, M. S. Cohen, W. P. Melega, A. P. Mulgaoonkar, A. DeSalles, B. Min, S. Y, “A review of low-intensity focused ultrasound pulsation,” *Brain Stimulation: Basic, Translational, and Clinical Research in Neuromodulation*, vol. 4, no. 3, pp. 125–136, Jul. 2011, doi: https://doi.org/10.1016/j.brs.2011.03.007.

[7] S. F. TAKAGI, SYOJI HIGASHINO, T. SHIBUYA, and N. OSAWA, “THE ACTIONS OF ULTRASOUND ON THE MYELINATED NERVE, THE SPINAL CORD AND THE BRAIN,” *The Japanese Journal of Physiology*, vol. 10, no. 2, pp. 183–193, Jan. 1960, doi: https://doi.org/10.2170/jjphysiol.10.183.

[8] J. M. Bronstein, M. Tagliati, R. L. Alterman, A. M. Lozano, J. Volkmann, A. Stefani, F. B. Horak, M. S. Okun, K, D. Foote, P. Krack, R. Pahwa, J. M. Henderson, M. I. Hariz, R. A. Bakay, A. Rezai, W. J. Marks, E. Moro, J. L. Vitek, F. M. Weaver, R. E. Gross, M. R. Delong, “Deep Brain Stimulation for Parkinson Disease,” *Archives of Neurology*, vol. 68, no. 2, Feb. 2011, doi: https://doi.org/10.1001/archneurol.2010.260.

[9] K. Venkatachalam and C. Montell, “TRP Channels,” *Annual Review of Biochemistry*, vol. 76, no. 1, pp. 387–417, Jun. 2007, doi: https://doi.org/10.1146/annurev.biochem.75.103004.142819.

[10] D. P. Darrow, P. O’Brien, T. J. Richner, T. I. Netoff, and E. S. Ebbini, “Reversible neuroinhibition by focused ultrasound is mediated by a thermal mechanism,” *Brain Stimulation*, vol. 12, no. 6, pp. 1439–1447, Nov. 2019, doi: https://doi.org/10.1016/j.brs.2019.07.015.

[11] “Welcome | MetaNeuron,” *www.metaneuron.org*. https://www.metaneuron.org/

[12] “Sim4Life,” *sim4life*, 2025. https://sim4life.swiss/

[13] M. W. Barnett and P. M. Larkman, “The action potential,” *Practical Neurology*, vol. 7, no. 3, pp. 192–197, Jun. 2007, Available: https://pn.bmj.com/content/7/3/192

[14] “Precision Acoustics - Ultrasound Acoustics,” *Precision Acoustics*. https://www.acoustics.co.uk/

[15] T. R. Wang, A. E. Bond, R. F. Dallapiazza, A. Blanke, D. Tilden, T. E. Hureta, S. Moosa, F. U. Prada, W. J. Elias, “Transcranial magnetic resonance imaging–guided focused ultrasound thalamotomy for tremor: technical note,” *Neurosurgical Focus*, vol. 44, no. 2, p. E3, Feb. 2018, doi: https://doi.org/10.3171/2017.10.focus17609.